Gamma-ray and multifrequency variability of blazars

Stefano Ciprini [1,2,3] (on behalf of the *Fermi* LAT collaboration)

(1) ASI Science Data Center, Frascati, Roma, Italy - (2) INAF, Astronomical Observatory of Rome, Monte Porzio Catone, Roma, Italy - (3) University of Perugia, Perugia, Italy

Abstract

Gamma-ray light curves and the gamma-ray variability properties of bright Fermi blazars are highlighted, and two examples of multiwavelength (MW) campaigns led by Fermi are reported: the first devoted to the new high-energy blazar PKS 1502+106 and the second to the eponymous blazar BL Lacertae. Variable blazars have weekly binned light curves that can be described by 1/f^a power density spectra (PDS) and show two kinds of gamma-ray variability: a rather constant baseline with sporadic flaring activity characterized by flatter PDS slopes resembling flickering and red noise with occasional intermittent activity, and, measured for a few blazars, strong activity-complex and structured temporal profiles characterized by long-term memory and steeper PDS slopes, reflecting a random walk mechanism. The two Fermi campaigns on single blazars reported here represent complementary studies. The first one is an example of a Target of Opportunity multifrequency campaign following the discovery and identification of a new gamma-ray flaring blazar (PKS 1502+106). The second one is an example of a planned multifrequency campaign catching, for the first time in gamma-rays, a well known source (BL Lacertae) in a non-flaring and rather low activity state.

Variable gamma-ray flux light curves

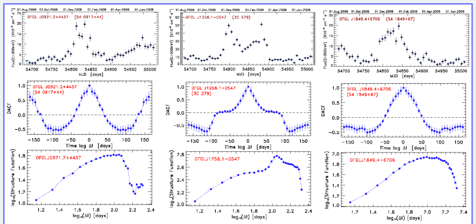

Figure 10. Example of DACF and SF functions applied to the weekly light curves of LBAS blazars They show different autocorrelation patterns, different zero lag peak amplitudes and crossing times, and different temporal power spectral trends and slopes, pointing out more different variability modes.

Abdo, A.A. et al. 2010, ApJ, 722, 520

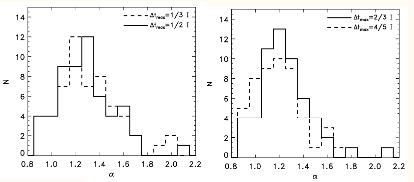

Figure 11. Distributions of the PDS power indices α for the weekly light curves of the 56 most bright and variable LBAS sources, selected as explained in the text. The values are obtained applying the SF considering four maximum lags (1/3, 1/2, top panel, and 2/3 and 4/5 bottom panel, of the total time range $I = t_{max} - t_{min}$). These distributions are peaked for values of the power index between 1.1 and 1.6.

Abdo, A.A. et al. 2010, ApJ, 722, 520

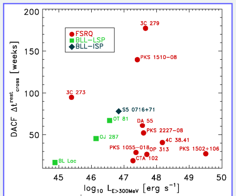

Figure scatter plot of the DACF crossing times in the rest frame of the source (corrected for z and beaming) vs. the total apparent isotropic γ-ray luminosity ($E > 300$ MeV) in the co-moving frame, defined as in the text, for 15 of the LBAS that are also part of the MOJAVE database. 3C 454.3 is out of the plot range (with $\Delta t^{cross}_{rest} = 254.3$ weeks and $\log_{10}(L_E) = 48.1$). All sources in this panel are labeled.

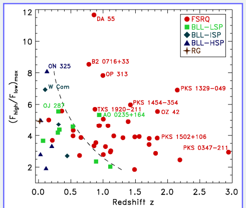

Figure scatter
plot of the maximum ratio of flux variations in adjacent weekly bins vs. the redshift for the same sources. A possible separation band between BL Lac objects and FSRQs is indicated by the line.

Abdo, A.A. et al. 2010, ApJ, 722, 520

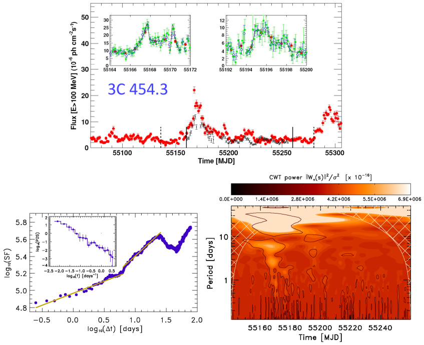

Figure 1. Light curve of the flux of 3C 454.3 in the 100 MeV–200 GeV band (red) between MJD 55,070–55,307 (2009 August 27–2010 April 21). The solid (dashed) lines mark the period over which the PSD (CWT) analysis has been conducted. The light curve of the 2008 July–August flare, shifted by 511 d, is shown for comparison (black). The insets show blow-ups of the two periods when the largest relative flux increases took place. The red, blue, and green data points in the insets correspond to daily, 6 hr, and 3 hr averaged fluxes, respectively. The fit results discussed are displayed as solid curves.

Top panel: SF of the 3 hr bin flux light curve for the period MJD 55,140–55,260 and corresponding PDS (inset). Bottom panel: plane contour plot of the continuous Morlet wavelet transform power density for the same light curve. Thick black contours are the 90% confidence levels of true signal features against white/red noise background, and cross-hatched regions represent the "cone of influence," where spurious edge effects become important.

Ackermann, M. et. al. 2010, ApJ, 721, 1383

Variable MW flux light curves

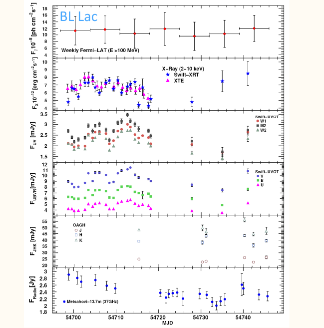

Figure 4. Simultaneous multifrequency flux light curves of BL Lac from the 48 days of an intensive *Fermi* campaign obtained with *Fermi*-LAT, *Swift*-XRT, and UVOT, OAGH, and Metsähovi observations. LAT weekly fluxes reported in the upper panel for this period are all TS > 10 detections. UV-to-near-IR fluxes are corrected for absorption.

Abdo, A.A. et al. 2011, ApJ, 730, 101

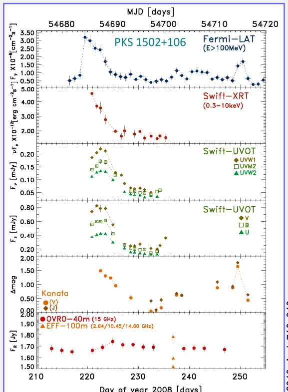

Figure 4. Simultaneous gamma-ray and multifrequency light curves obtained during the multiwavelength campaign of 2008 August triggered by the high-energy outburst discovered by *Fermi* LAT. The flux above 100 MeV, the X-ray flux (0.3–10 keV) by *Swift*-XRT, the six-band fluxes monitored by *Swift*-UVOT, the Kanata-TRISPEC differential relative magnitude light curves (optical ΔV and near-IR ΔJ bands) and corresponding measures of the linear polarization degree, and the 15 GHz radio light curve from OVRO 40 m are reported.

Abdo, A.A. et al. 2010, ApJ, 710, 810

Variable MW SEDs

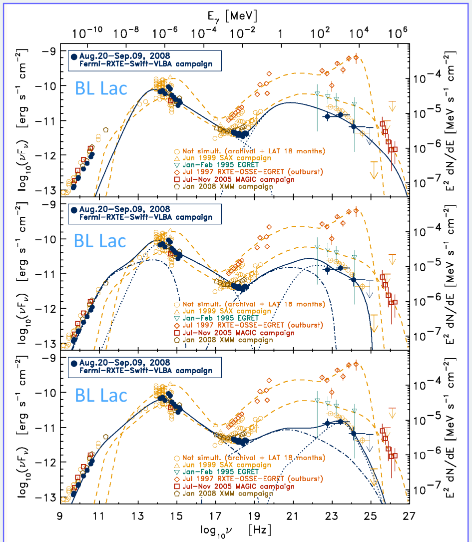

Figure 10. 2008 August 20–September 9 simultaneous SED of BL Lac assembled with data from the coordinated campaign, and some archival data from the literature for comparison. The data are modeled with a single-zone pure-SSC (top panel), two-zone pure SSC description (center panel), and a single-zone SSC plus ERC descriptions (bottom panel). In the two-zone pure SSC description, the blue/dark dotted line represents the compact, faster, and high-energy emission component, while the blue/dark dash-dotted line is the larger and diluted zone emission component. In the SSC plus ERC model, the blue/dark is the ERC emission (disk emission negligible here) component and the blue/dark dash-dotted line is the synchrotron and SSC emission component. Past published and archival data are taken from Böttcher & Bloom (2000), Ravasio et al. (2002), Böttcher et al. (2003), Albert et al. (2007), and Raiteri et al. (2009), and fit models for two of these past epochs (the 1997 outburst campaign and the 2005 campaign; Ravasio et al. 2002; Albert et al. 2007) are represented as orange/clear long-dashed lines in each panel.

Abdo, A.A. et al. 2011, ApJ, 730, 101

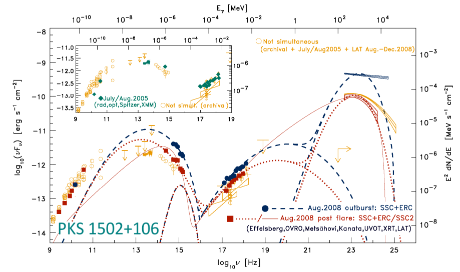

Figure 11. Major panel: overall radio-to-gamma-ray SED of PKS 1502+106 assembled with data from the two-week *Fermi* LAT multifrequency campaign of 2008 August. The two representative, time-averaged, states for this campaign (time intervals outlined in Figure 2), i.e., the high state (2008 August 5–10, DOY 2008: 218.95–224.0; blue filled circle symbol), and the post-flare (intermediate brightness) state (2008 August 11–22; DOY 2008: 224.0–235.42; red filled square symbol), are represented along with their SSC and ERC model attempts. Archival non-simultaneous data (including the 2005 July–August data, and the whole four-month cumulated LAT spectrum, open orange circle symbols and strip) are reported in the background for comparison. The high Compton dominance and gamma-ray bolometric luminosity reached during the outburst is evident. The SED of the outburst state is reported with a superposed one-zone "SSC+ERC" model fit attempt (where the SSC dominates the radio-to-X-ray SED and the ERC produces the gamma-ray component, blue dashed line), while the SED of the post-flare state is reported with two possible models superposed: the same SSC+ERC modeling (SSC radio-to-X-ray and ERC for gamma-ray band, red dotted line) and also a pure one-zone SCC attempt (labeled with "SSC2," a second type of stand-alone SSC model for the entire radio-to-gamma-ray SED, continuous red line). Inset panel: the 2005 July–August non-simultaneous SED (filled orange circles) assembled with the *XMM-Newton* EPIC-MOS data from 2005 July 17, the *Spitzer* IRS observation from 2005 August 13, radio flux data from Metsähovi and RATAN radio observatories, and optical data from the Catalina Sky Survey. Archival non-simultaneous data (open circles) are reported in background. This two-month averaged SED is consistent with a low or mildly active stage (suggested by the X-ray flux above 1×10^{-12} erg cm^{-2} s^{-1}) and can still be explained by a pure one-zone SSC model.

Abdo, A.A. et al. 2010, ApJ, 710, 810

References

- Abdo, A.A. et al. 2011, ApJ, 730, 101
- Abdo, A.A. et al. 2010, ApJ, 722, 520
- Abdo, A.A. et al. 2010, ApJ, 716, 30
- Abdo, A.A. et al. 2010, ApJ, 710, 810
- Ackermann, M. et. al. 2010, ApJ, 721, 1383
- Ciprini, S., et al. 2010, ASP Conf. Ser. 427, 293
- Ciprini, S., 2010, AIP Conf. Proc., 1248, 409